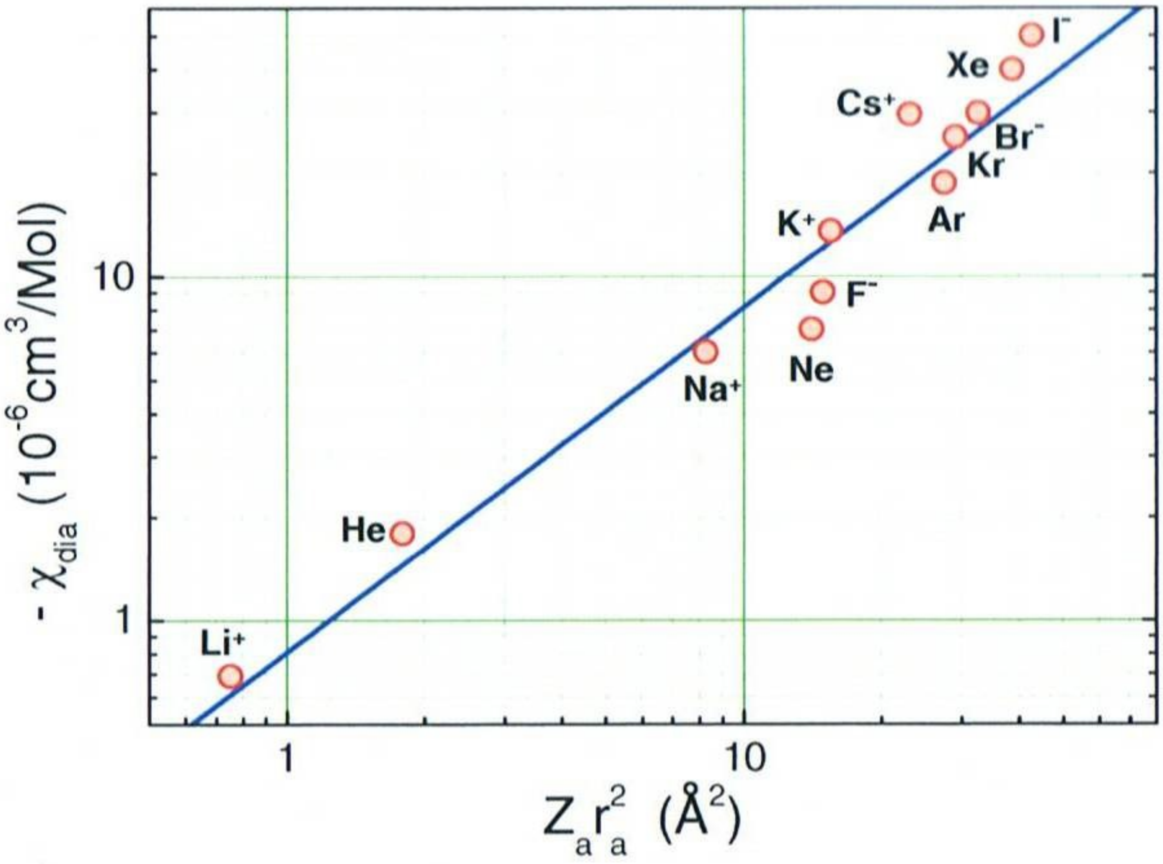

Abbildung 12.2: Molare diamagnetische Suszeptibilität von Atomen und Ionen mit abgeschlossener Elektronenschale aufgetragen gegen $Z_a r_a^2$. Die Suszeptibilität eines Gases oder Festkörpers, der aus diesen Atomen oder Ionen zusammnegesetzt ist, erhält man, indem man mit der Dichte in mol/cm^3 multipliziert. Um in SI-Einheiten zu konvertieren, muss man mit 4π multiplizieren.

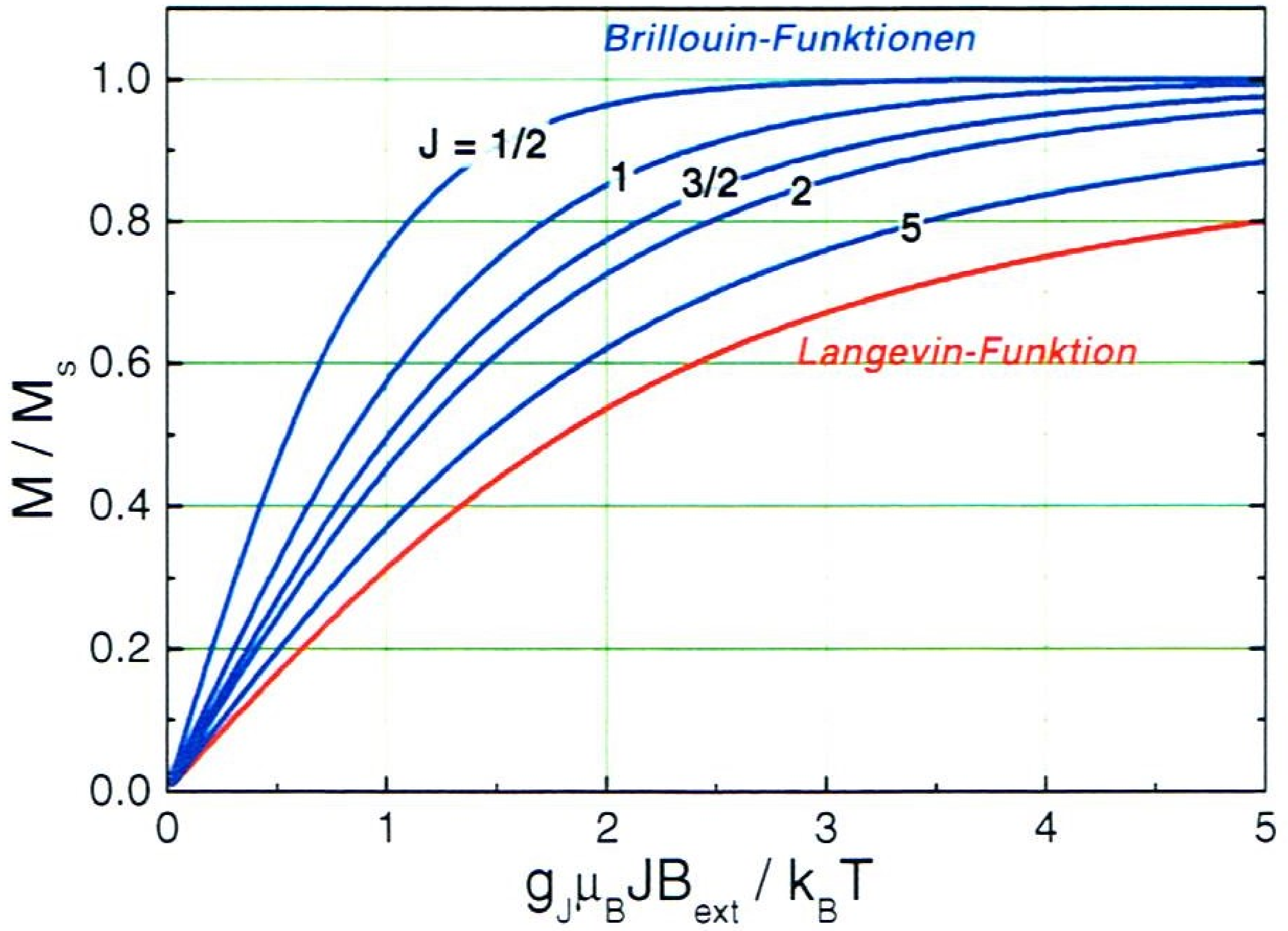
Brillouin-Funktionen
J = 1/2
1
3/2
2
5
Langevin-Funktion
M / M_s
0.0
0.2
0.4
0.6
0.8
1.0
0
1
2
3
4
5
$g_J \mu_B J B_{ext} / k_B T$

Rare Earth Metals and Ions

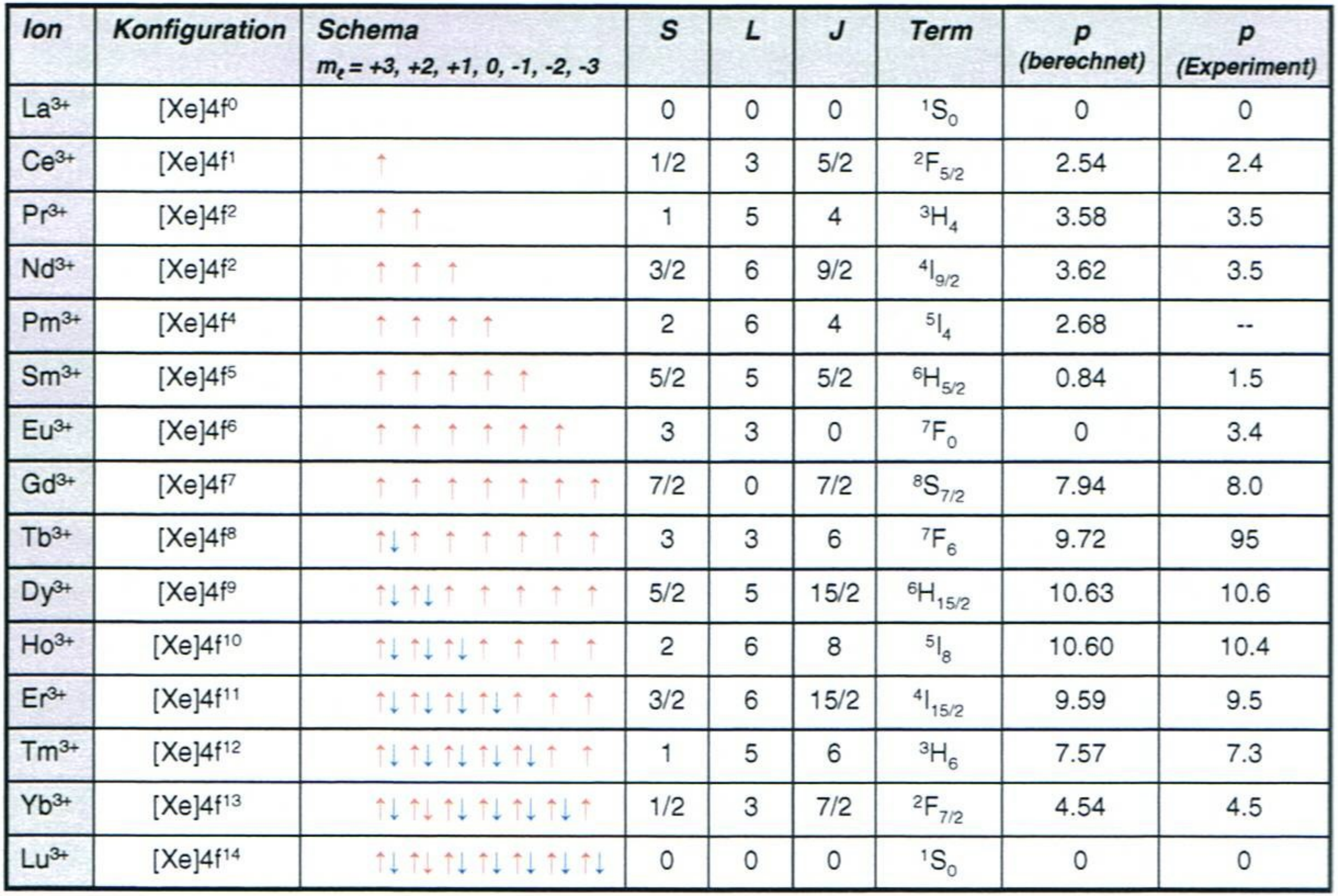

Ion	**Konfiguration**	**Schema** m_ℓ = +3, +2, +1, 0, -1, -2, -3	**S**	**L**	**J**	**Term**	**p** (berechnet)	**p** (Experiment)
La^{3+}	$[Xe]4f^0$		0	0	0	$^1S_0$	0	0
Ce^{3+}	$[Xe]4f^1$	↑	1/2	3	5/2	$^2F_{5/2}$	2.54	2.4
Pr^{3+}	$[Xe]4f^2$	↑ ↑	1	5	4	$^3H_4$	3.58	3.5
Nd^{3+}	$[Xe]4f^2$	↑ ↑ ↑	3/2	6	9/2	$^4I_{9/2}$	3.62	3.5
Pm^{3+}	$[Xe]4f^4$	↑ ↑ ↑ ↑	2	6	4	$^5I_4$	2.68	--
Sm^{3+}	$[Xe]4f^5$	↑ ↑ ↑ ↑ ↑	5/2	5	5/2	$^6H_{5/2}$	0.84	1.5
Eu^{3+}	$[Xe]4f^6$	↑ ↑ ↑ ↑ ↑ ↑	3	3	0	$^7F_0$	0	3.4
Gd^{3+}	$[Xe]4f^7$	↑ ↑ ↑ ↑ ↑ ↑ ↑	7/2	0	7/2	$^8S_{7/2}$	7.94	8.0
Tb^{3+}	$[Xe]4f^8$	↑↓ ↑ ↑ ↑ ↑ ↑ ↑	3	3	6	$^7F_6$	9.72	95
Dy^{3+}	$[Xe]4f^9$	↑↓ ↑↓ ↑ ↑ ↑ ↑ ↑	5/2	5	15/2	$^6H_{15/2}$	10.63	10.6
Ho^{3+}	$[Xe]4f^{10}$	↑↓ ↑↓ ↑↓ ↑ ↑ ↑ ↑	2	6	8	$^5I_8$	10.60	10.4
Er^{3+}	$[Xe]4f^{11}$	↑↓ ↑↓ ↑↓ ↑↓ ↑ ↑ ↑	3/2	6	15/2	$^4I_{15/2}$	9.59	9.5
Tm^{3+}	$[Xe]4f^{12}$	↑↓ ↑↓ ↑↓ ↑↓ ↑↓ ↑ ↑	1	5	6	$^3H_6$	7.57	7.3
Yb^{3+}	$[Xe]4f^{13}$	↑↓ ↑↓ ↑↓ ↑↓ ↑↓ ↑↓ ↑	1/2	3	7/2	$^2F_{7/2}$	4.54	4.5
Lu^{3+}	$[Xe]4f^{14}$	↑↓ ↑↓ ↑↓ ↑↓ ↑↓ ↑↓ ↑↓	0	0	0	$^1S_0$	0	0

Ground state multiplets according to Hund's rules for the 3+ ions of the 4f series

Rare Earth Metals and Ions

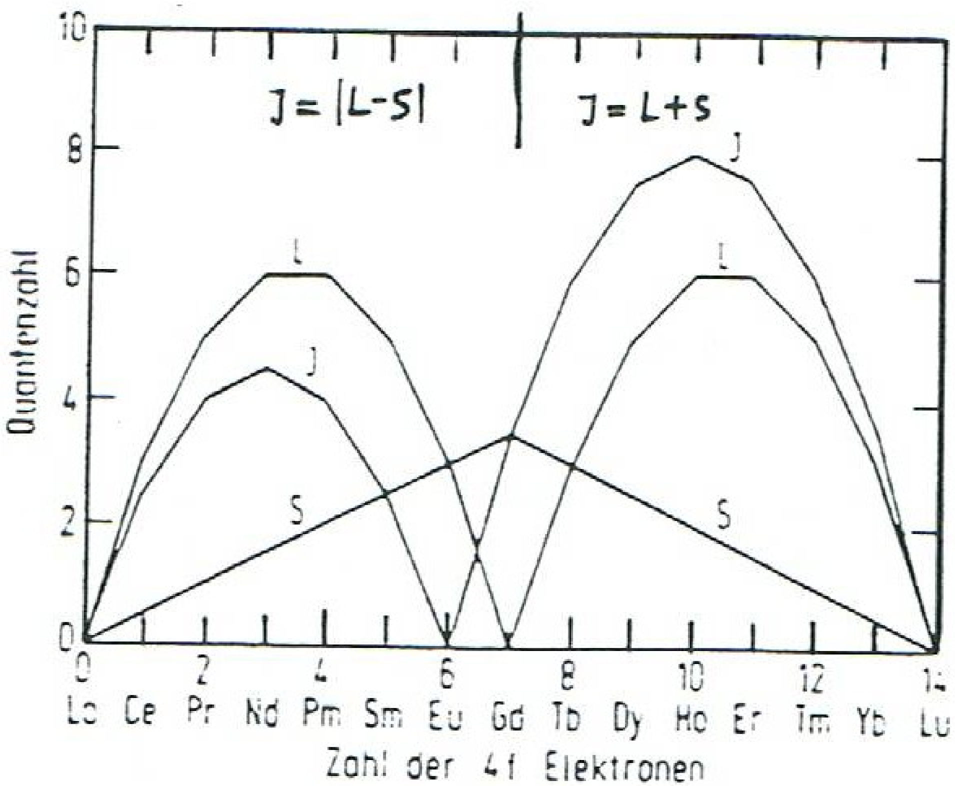

Spin S, orbital angular momentum, L and total angular momentum J according to Hund’s rules for the 3+ ions of the 4f series.

Rare Earth Metals and Ions

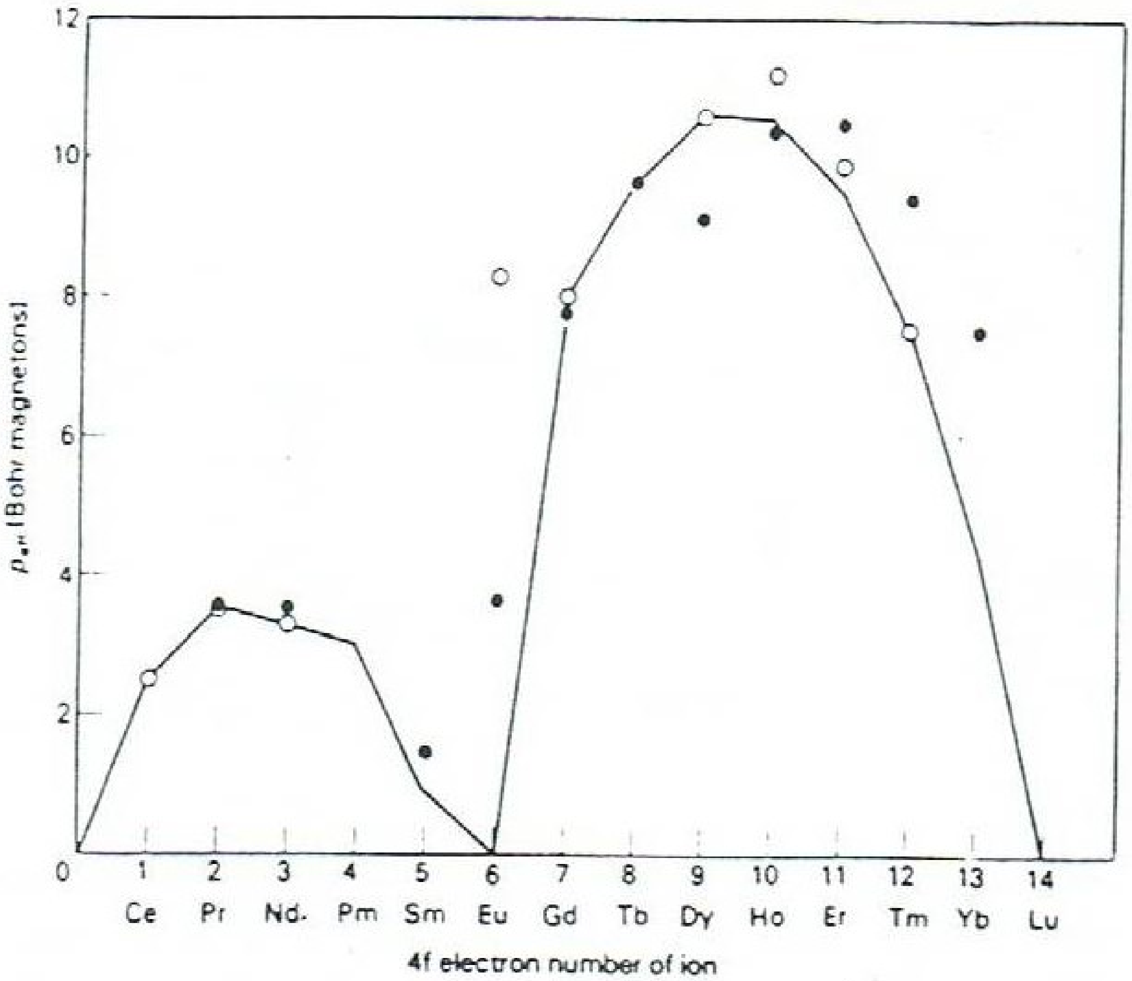

Comparison of measured effective magnetic moments and calculated values for the 4f series of rare earth metals.

3d- Transition Metal Ions

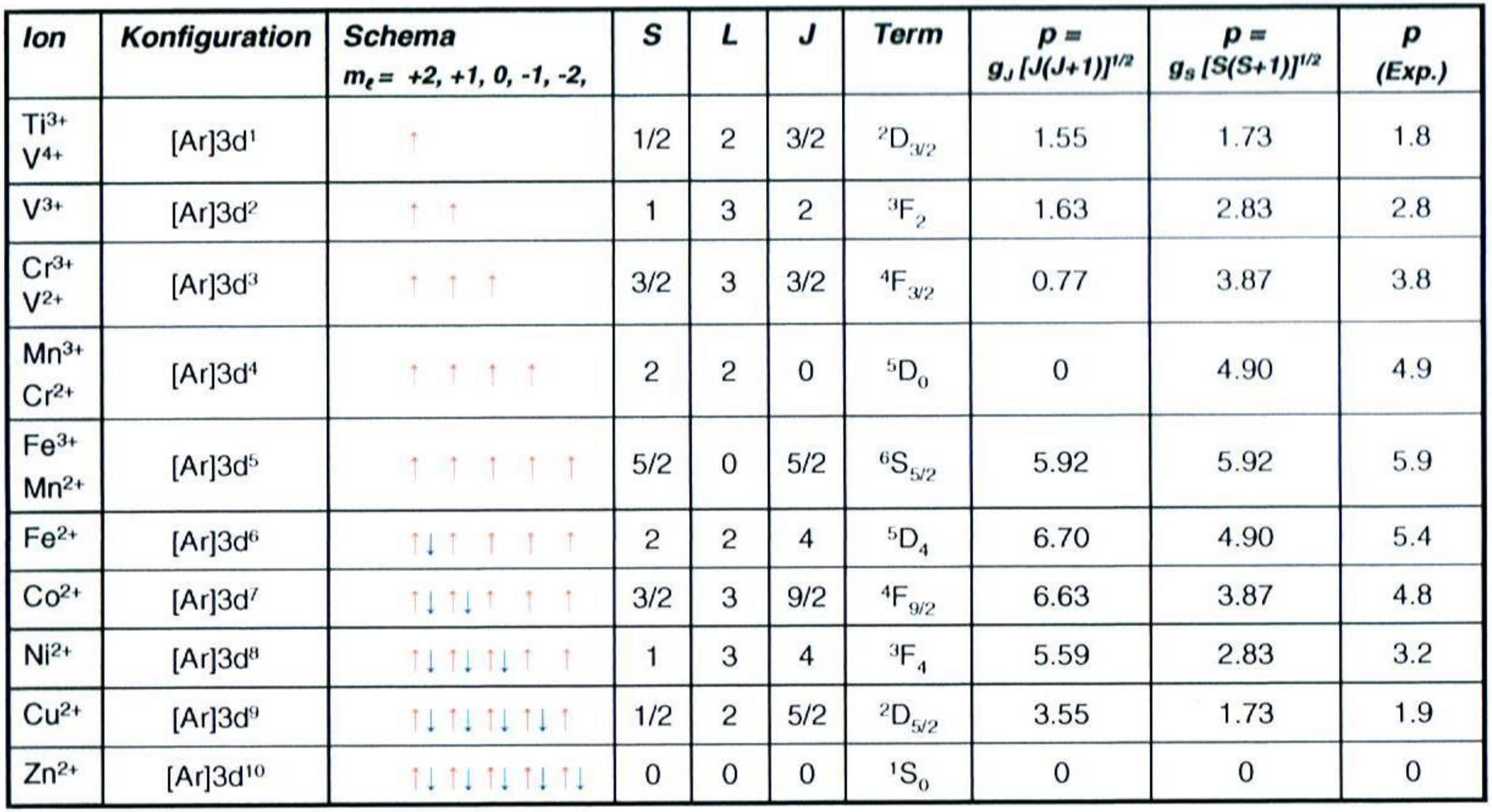

Ion	Konfiguration	Schema $m_\ell =$ +2, +1, 0, -1, -2,	S	L	J	Term	$p = g_J [J(J+1)]^{1/2}$	$p = g_S [S(S+1)]^{1/2}$	p (Exp.)
Ti^{3+} V^{4+}	[Ar]3d^1	↑	1/2	2	3/2	${}^2D_{3/2}$	1.55	1.73	1.8
V^{3+}	[Ar]3d^2	↑ ↑	1	3	2	${}^3F_2$	1.63	2.83	2.8
Cr^{3+} V^{2+}	[Ar]3d^3	↑ ↑ ↑	3/2	3	3/2	${}^4F_{3/2}$	0.77	3.87	3.8
Mn^{3+} Cr^{2+}	[Ar]3d^4	↑ ↑ ↑ ↑	2	2	0	${}^5D_0$	0	4.90	4.9
Fe^{3+} Mn^{2+}	[Ar]3d^5	↑ ↑ ↑ ↑ ↑	5/2	0	5/2	${}^6S_{5/2}$	5.92	5.92	5.9
Fe^{2+}	[Ar]3d^6	↑↓ ↑ ↑ ↑ ↑	2	2	4	${}^5D_4$	6.70	4.90	5.4
Co^{2+}	[Ar]3d^7	↑↓ ↑↓ ↑ ↑ ↑	3/2	3	9/2	${}^4F_{9/2}$	6.63	3.87	4.8
Ni^{2+}	[Ar]3d^8	↑↓ ↑↓ ↑↓ ↑ ↑	1	3	4	${}^3F_4$	5.59	2.83	3.2
Cu^{2+}	[Ar]3d^9	↑↓ ↑↓ ↑↓ ↑↓ ↑	1/2	2	5/2	${}^2D_{5/2}$	3.55	1.73	1.9
Zn^{2+}	[Ar]3d^{10}	↑↓ ↑↓ ↑↓ ↑↓ ↑↓	0	0	0	${}^1S_0$	0	0	0

Ground state multiplets according to Hund’s rules for the 2+ ions of the 3d series

3d- Transition Metal Ions

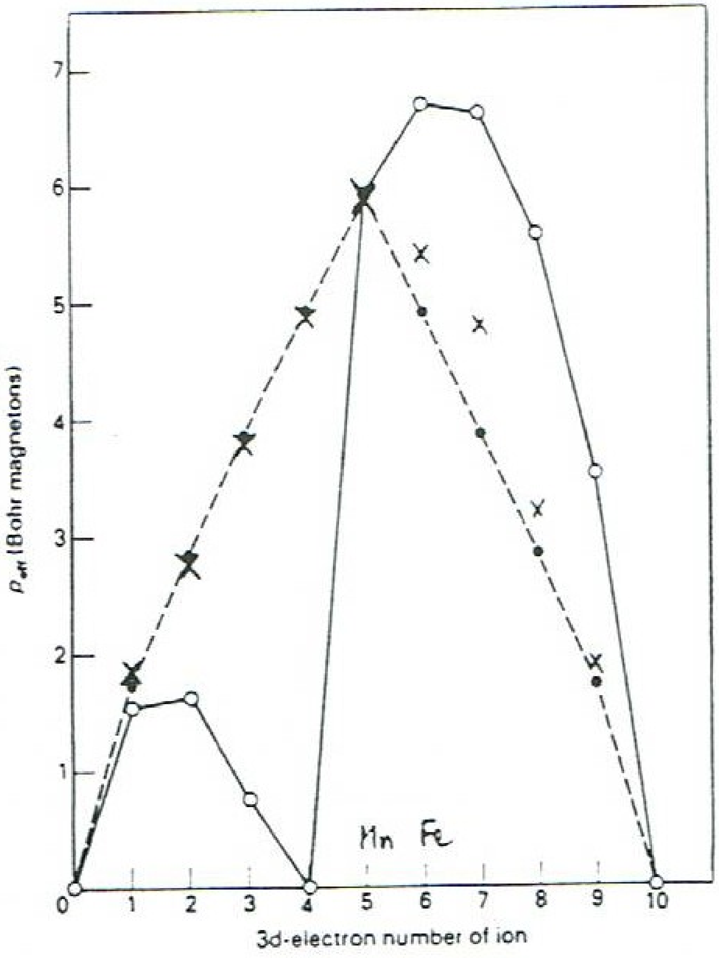

Comparison of measured effective magnetic moments and calculated values for the 3d series of transition metals. Neglecting L describes the experimental data better.

3d- Transition Atoms and Metals

Table 7.2. Number of 3*d* and 4*s* electrons in the free transition metal atoms

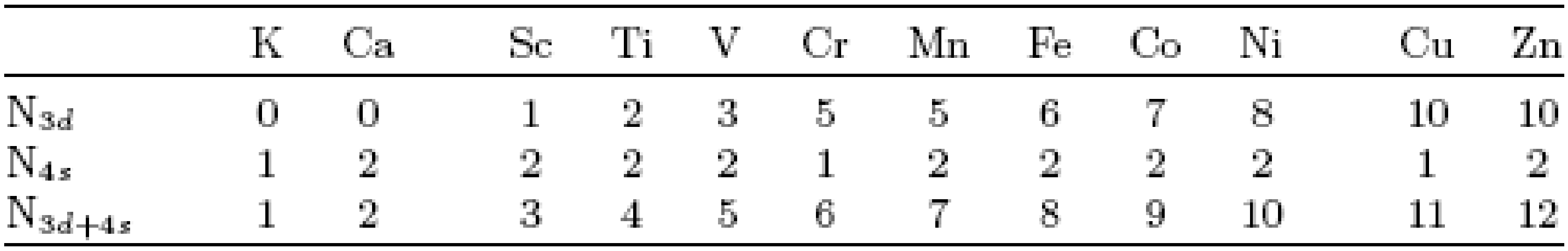

	K	Ca	Sc	Ti	V	Cr	Mn	Fe	Co	Ni	Cu	Zn
N_{3d}	0	0	1	2	3	5	5	6	7	8	10	10
N_{4s}	1	2	2	2	2	1	2	2	2	2	1	2
N_{3d+4s}	1	2	3	4	5	6	7	8	9	10	11	12

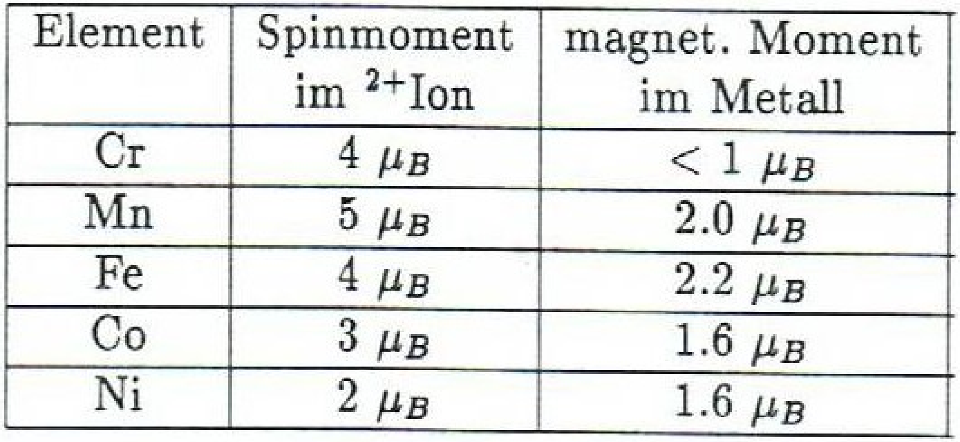

Element	Spinmoment im $^{2+}$Ion	magnet. Moment im Metall
Cr	4 μ_B	$< 1\ \mu_B$
Mn	5 μ_B	2.0 μ_B
Fe	4 μ_B	2.2 μ_B
Co	3 μ_B	1.6 μ_B
Ni	2 μ_B	1.6 μ_B

Magnetic moments of 3d transition metals compared to spin moment according to Hund’s rules.

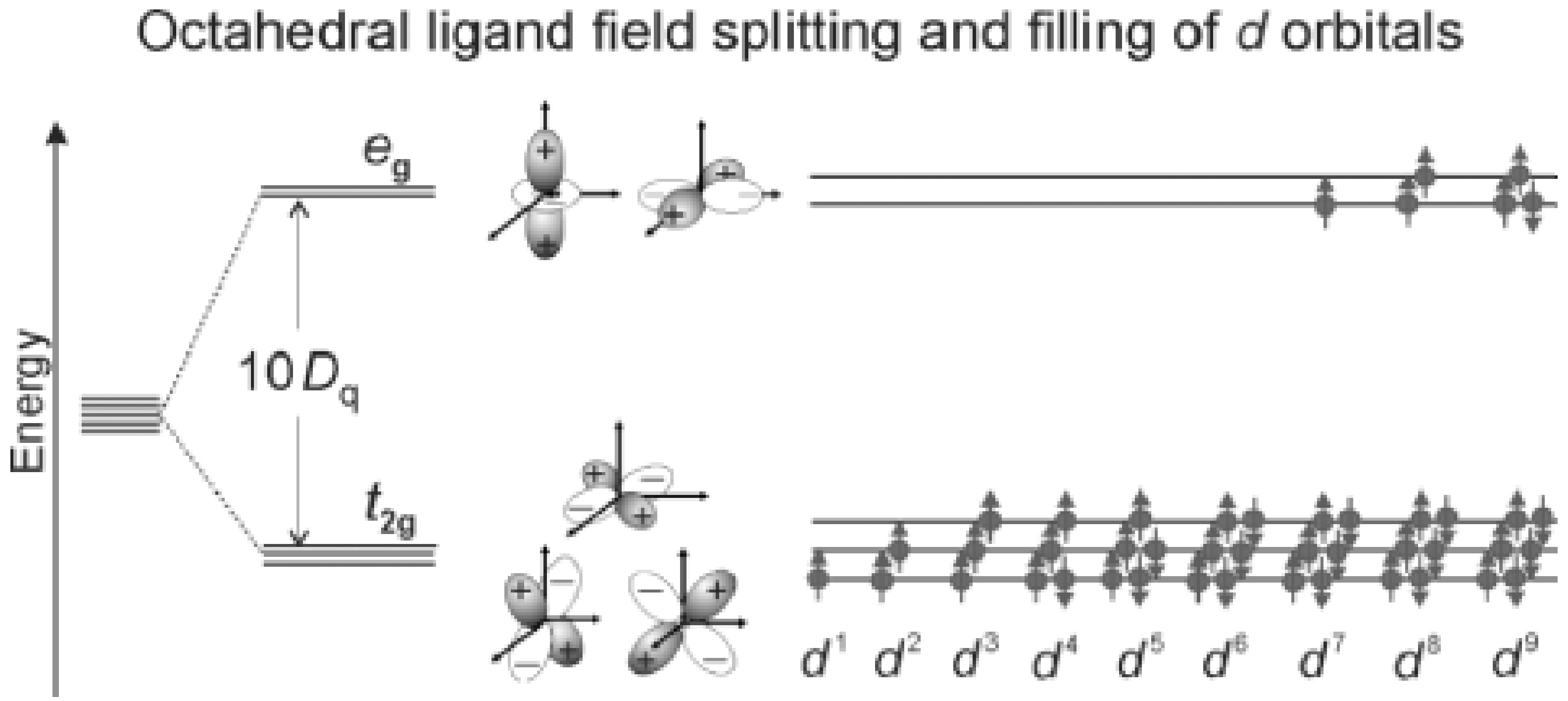

Fig. 6.13. Splitting of the d shell in an octahedral ligand field into doubly degenerate e_g and triply degenerate t_{2g} states. Also shown is the filling of the energy levels for the case that the e_g–t_{2g} splitting is large relative to the exchange interaction [204]. The resulting ground states for $d^4 - d^7$ are called the *low-spin* configurations (see Sect. 7.5.1)

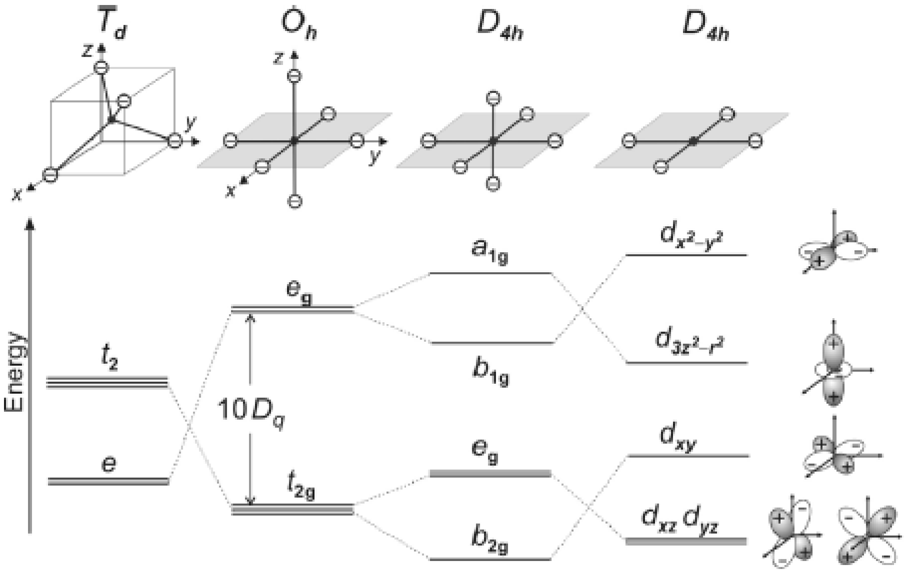

Fig. 7.9. Ligand field splitting of energy levels for a single d electron in fields of different coordination and symmetry. For the cases shown the central $3d$ ion is assumed to be coordinated by electronegative ligands such a oxygen. On the left we compare the splitting in the tetrahedral (T_d) and octahedral O_h cubic symmetries. For octahedral O_h and tetragonal D_{4h} symmetries we have assumed equal interaction strengths in the $x-y$ plane and varied the interaction along z, as illustrated. On the right are plotted the orbital densities $(d_i)^2$ of the LF eigenfunctions d_i and the numerical sign of d_i wavefunction lobes are indicated on top of the charge densities

3d- Transition Metal Ions

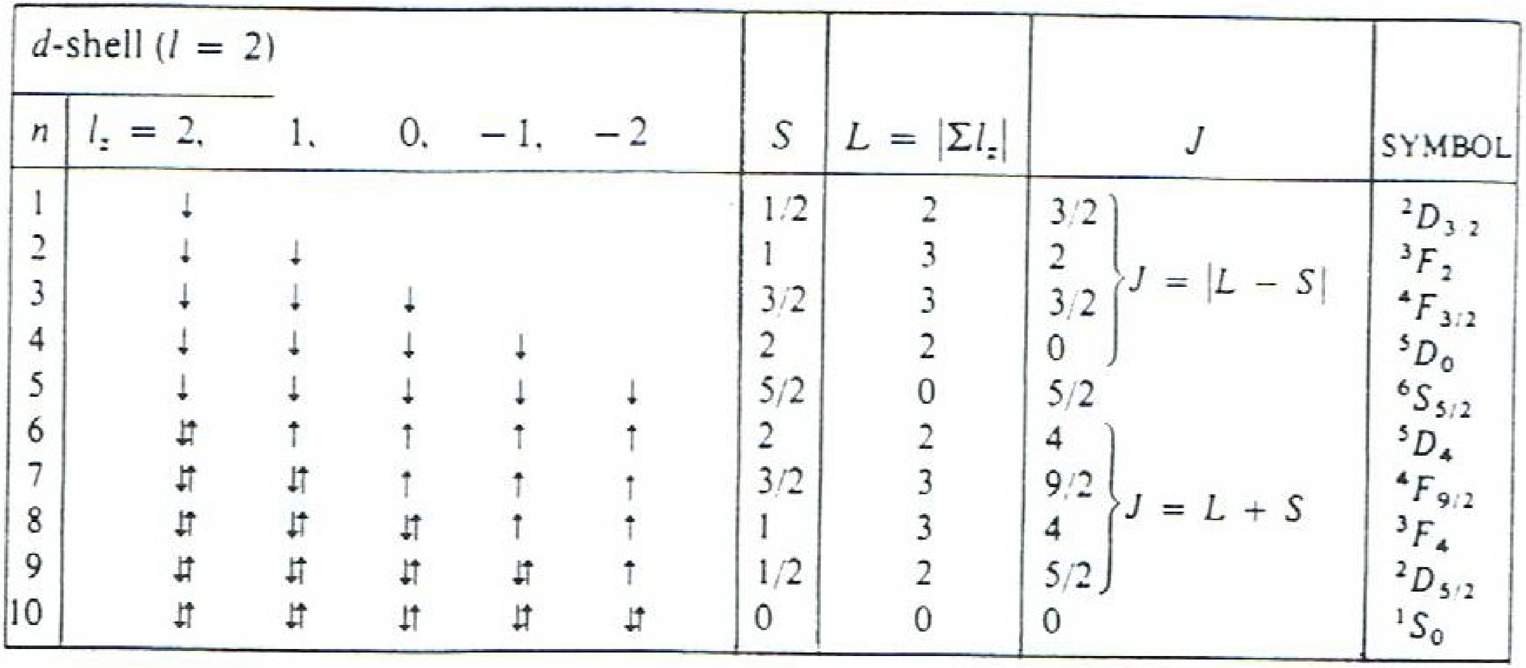

d-shell (l = 2)										
n	$l_z = 2,$	1,	0,	−1,	−2	S	$L = \lvert \Sigma l_z \rvert$	J		SYMBOL
1	↓					1/2	2	3/2	$J = \lvert L - S \rvert$	$^2D_{3/2}$
2	↓	↓				1	3	2		$^3F_2$
3	↓	↓	↓			3/2	3	3/2		$^4F_{3/2}$
4	↓	↓	↓	↓		2	2	0		$^5D_0$
5	↓	↓	↓	↓	↓	5/2	0	5/2		$^6S_{5/2}$
6	⇅	↑	↑	↑	↑	2	2	4	$J = L + S$	$^5D_4$
7	⇅	⇅	↑	↑	↑	3/2	3	9/2		$^4F_{9/2}$
8	⇅	⇅	⇅	↑	↑	1	3	4		$^3F_4$
9	⇅	⇅	⇅	⇅	↑	1/2	2	5/2		$^2D_{5/2}$
10	⇅	⇅	⇅	⇅	⇅	0	0	0		$^1S_0$

Ground state multiplets according to Hund’s rules for the 2+ ions of the 3d series he.

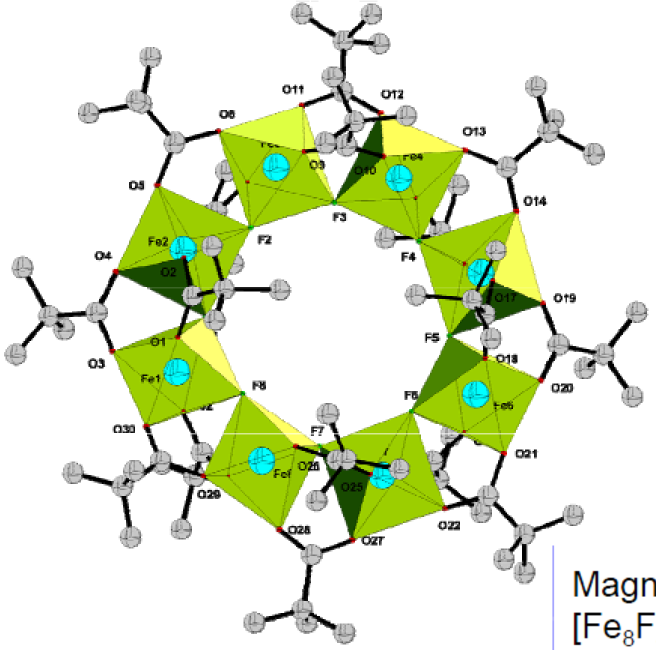

Magnetische Suszeptibilitätsmessung von $[Fe_8F_8(Bu^t\text{-}COO)_{16} \cdot (CH_3)_2CO]$,2 K - 300 K, B=1T

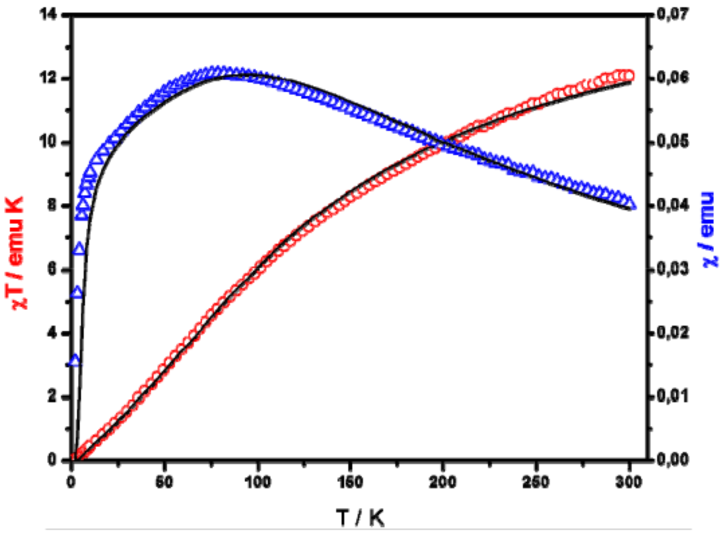

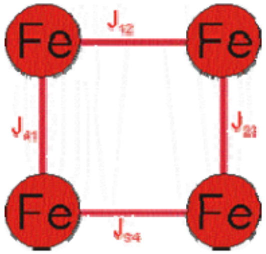

B / T	1
S g	5/2 1,95
$J_{1,2}$ / cm^{-1}	-5,98

χT_{300K} = 12,1 emuK